

KINETICS OF OXIDATION OF SILICON BY ELECTRON CYCLOTRON RESONANCE PLASMAS

J. Joseph, Y.Z. Hu* and E.A. Irene*

Department of Physics and Chemistry
Ecole Centrale de Lyon, 69130 Ecully, France.

*Department of Chemistry
University of North Carolina
Chapel-Hill, NC 27599-3290

ABSTRACT

In-situ ellipsometry, both single wavelength and spectroscopic, has been used to study the electron cyclotron resonance plasma oxidation of Si. Spectroscopic ellipsometry has been used to establish that the best fit optical model for the oxidation is a two layer model where the interface layer forms early and stabilizes and the outer layer is SiO₂. The interface layer is modeled well as a mixture of a-Si and oxide. The kinetics of film growth were followed using single wavelength ellipsometry at a temperature insensitive wavelength, and the results were in agreement with the Cabrera-Mott theory.

INTRODUCTION

Low temperature processing is required for the development of silicon technology. For this purpose Electron Cyclotron Resonance (ECR) plasma appears to be a promising tool. The most interesting feature of this method is that the high ionization ratio of the plasma is associated with low energy ionic species. Therefore, it is possible to obtain high quality films without the damage associated with impinging ionic species. The use of plasmas to grow SiO₂ films dates from the beginning of Si technology^{1,2,3}, but the process usually included elevated temperatures either during and/or after plasma treatment. A number of studies on ECR plasma oxidation are available^{4,5,6,7,8}. In the latest of these studies⁸, among the many experimental parameters examined, applied bias voltage effects and electronics quality of the oxides was studied, and these issues overlap with the present study and will be discussed further.

Since the ECR plasma technique enables the fabrication of thin oxides at low temperatures, the present study is aimed at the understanding of the oxidation mechanism

of Si between about 80°C and 400°C. In order to obtain a reliable description of the kinetics of the oxidation, in-situ during process ellipsometric measurements were used in two complementary ways: static spectroscopic and dynamic real time at a fixed wavelength. From the resulting experimental data the main features of the oxide layer are extracted using a two layer optical model^{9,10}.

EXPERIMENTAL PROCEDURES

A specially designed high precision spectroscopic ellipsometer was constructed with an independent process chamber^{11,12}. The ellipsometer was a rotating analyzer system with a Xenon lamp allowing a spectral range between 2.5 eV and 4.5 eV. This range was chosen because it contains the main features of the dielectric function of silicon, viz. the two interband transitions at 3.4 eV and 4.2 eV. One of the main problems with performing in-situ ellipsometry is the unavailability of reliable optical properties versus temperature data. In order to circumvent this difficulty, we obtained the spectrum at room temperature after cooling the sample, and at the oxidation temperature we performed the real time kinetics measurements at a specific wavelength. These latter measurements were carried out using 340 nm (3.65 eV) light. This energy was chosen because we found that the spectra measured at different temperatures are nearly coincident at this energy⁹. Thus, at 340 nm we are able to ignore the temperature changes in the optical properties of Si and obtain the changing thickness of the oxide layer. Moreover, for the thin oxides on Si at this wavelength the accuracy of the rotating analyzer system is good.

The process chamber was equipped with a home-made electron cyclotron resonance source operating at 300 W and at 2.45 GHz. For this study the oxygen pressure was 5×10^{-4} torr and the distance between the mouth of the microwave cavity and the sample was 20 cm. The sample was heated by a light source located at the backside of the sample stage, and temperature was controlled by a thermocouple. The sample holder was electrically isolated from the chamber and a bias voltage between the sample and the plasma cavity was controlled by an independent power supply.

OPTICAL MODELLING

The physical parameters of the oxide layers are extracted both from the single wavelength and spectroscopic ellipsometric measurements using optical models. In order to interpret the single wavelength measurements in terms of SiO₂ thickness versus oxidation time, a simple one layer model was used. From a comparison of the theoretical trajectory corresponding to the growth of a layer with the experimental points, a thickness was obtained for each experimental point. For the spectra consisting of 41 data points between 2.5 and 4.5 eV, a stratified two layer model was used. Each layer is either a medium for which the optical properties are known, such as SiO₂, or where the properties can be described by a mixture of components. For this later case, the optical properties are determined from the dielectric functions of the components and the volume fraction using the Bruggeman effective medium approximation, BEMA¹³. To limit the number of parameters to be determined to four, we assumed that the entire oxide layer can be described by no more than two layers and that each layer was composed of no more than two components. The layers were assumed to be composed of one or two of the following components with well known dielectric functions: c-Si¹⁴, a-Si¹⁵, SiO₂¹⁶ and voids. Four reasonable models shown in Figure 1 were evaluated and the results are summarized in Table 1 for a typical sample. From column 2 which shows the quality of the fit in term of an unbiased estimator⁹, δ , model 4 yields the best fit. This model yields an a-Si volume fraction, f_v , of near 50% for the interface layer, and the relevant parameters are the thicknesses of the top SiO₂ film, L_{ox} , and the interface layer, L_{int} .

DTIC QUALITY INSPECTED 4

For	
I	<input checked="" type="checkbox"/>
1	<input type="checkbox"/>
on	<input type="checkbox"/>
on/	
ty Codes	
and/or	
cial	

A-1

EXPERIMENTAL RESULTS

The ECR plasma oxidation of Si was studied at different sample bias and temperature conditions. We found that an applied sample bias of -30 V halted the film growth, and the plasma became unstable above 60 V. Thus our investigation was between these values.

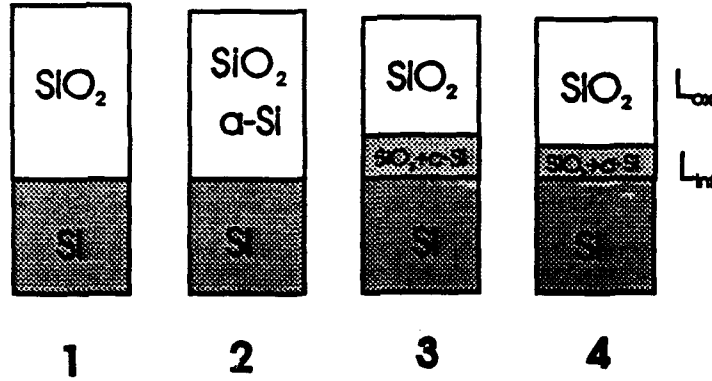


Figure 1. Optical models considered.

Table 1. Comparison of the optical models.

MODEL	$\delta \times 10^4$	L_{ox} (nm)	L_{int} (nm)	f_v (c-Si or a-Si) %
1	167	10.6 ± 0.5	\	\
2	104	9.6 ± 0.4	\	4.6 ± 1.5
3	115	7.6 ± 1.5	2.0 ± 0.7	39 ± 60
4	48	7.8 ± 0.3	2.2 ± 0.2	54 ± 4

Figure 2 shows the evolution of the ellipsometric parameters, Δ and Ψ , during the first 20 min of room temperature oxidation. In this Figure the solid line corresponds to a calculation performed with a one layer model (model 1 in Figure 1). From these results along with spectroscopic measurements, it appears that two different oxidation regimes occur during plasma oxidation. The first regime corresponds to about the first five degrees shift of Δ downwards, or about 2 nm in oxide thickness. The general behavior of the trajectories suggests that the ion bombardment is the main effect. The second oxidation regime corresponds to the growth of the SiO_2 film. During this period the experimental points are close to the theoretical line for an SiO_2 on Si layer. The different trajectories used for fitting were calculated using different refractive indexes for the SiO_2 layer. Spectroscopic measurements were performed during this second regime and were analyzed using Model 4 yielding L_{ox} and L_{int} values. The evolution of these parameters is shown in Figure 3. The interface layer was always found to be composed of nearly 50 % a-Si and 50 % SiO_2 . These results show that the interface layer forms during the first stage of

oxidation and remains almost constant during the growth of the oxide layer.

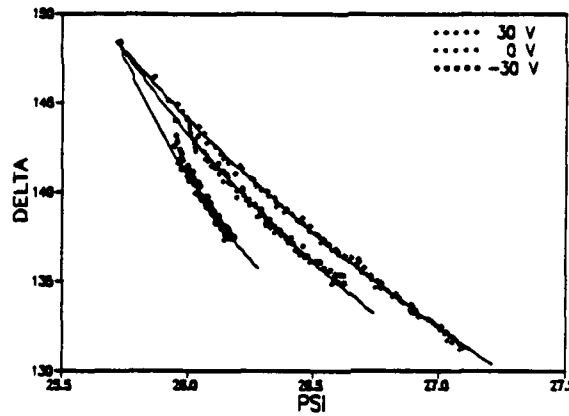


Figure 2. Evolution of the Δ, Ψ trajectories with oxidation.

Studies of oxidation were also done at four substrate temperatures (50°C, 200°C, 300°C, 400°C) at a bias of 30 V. The shape of the film thickness versus time data is similar for all the temperatures. However, for the longest times or the thicker oxides the unbiased estimator of the fitting procedure increases showing the limitation of the optical model.

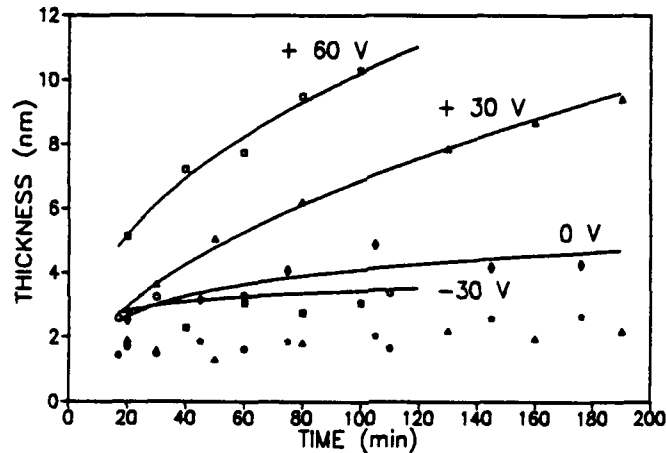


Figure 3. Results of two layer modelling of spectroscopic measurements. Open symbols represent oxide thickness, solid symbols represent interface thickness.

DISCUSSION OF RESULTS

For thermal oxidation of Si there exists significant evidence that the linear parabolic oxidation model is a reasonable approximation to the kinetics¹⁷. In the ECR plasma oxidation at low temperature the moving species are most likely different from those for thermal oxidation and the transport of these species is not only due to diffusion, but also and more importantly to the drift of charged species in the electric field. Many of these

kind of models also yield a linear parabolic rate law¹⁸. In order to check the consistency of such an approach, the oxide thickness versus the square root of the time for the growth of one of our thicker oxides is plotted in Figure 4.

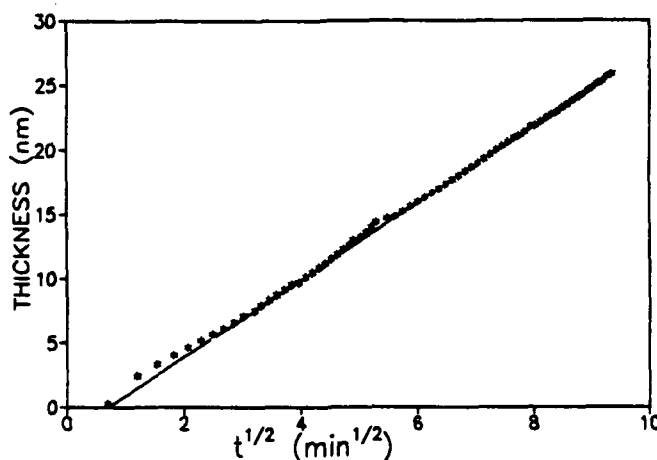


Figure 4. Thickness of the oxide layer as a function of the square root of ECR oxidation time obtained at 300°C for 30 V applied bias.

After the first few data points the results fit the $t^{1/2}$ dependence. Thus our results are interpreted with the simple relationship:

$$L^2 = Bt + C$$

where L and t are the oxide thickness and the oxidation time, respectively, and B and C are constants. Parabolic behavior was also reported in a previous ECR oxidation study⁸ for the early regime. All the data fit to this equation gave insignificant values for C . Thus only B was used for comparison with the model. Therefore, using the total thickness $L_t = L_{ox} + L_{ms}$ as the thickness of the layer, Figures 5 and 6 show the kinetics data and the linear fits which provide the parabolic coefficient B .

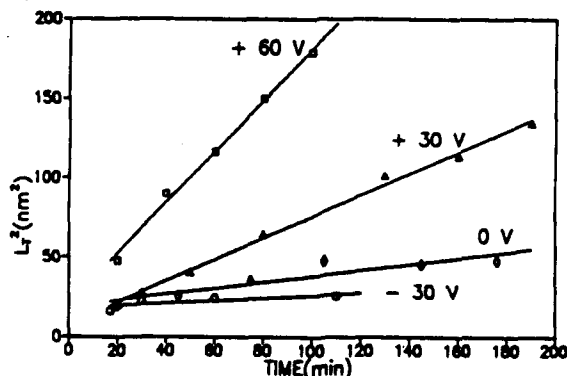


Figure 5. Growth law for four applied bias voltages.

Using the Cabrera-Mott theory¹⁷ for oxidation by charged species in the limit of the low field, the growth rate law is given by:

$$L^2 = C_1 \exp\left(-\frac{E_a}{kT}\right) \cdot \frac{V_{ox} t}{kT} + C_2$$

where C_1 and C_2 are constants, V_{ox} is the potential drop across the oxide film, E_a is the activation energy for diffusion, t is the oxidation time, T is the temperature, and k is the Boltzman constant. In order to compare our results to this theory, the dependance of our experimental parabolic coefficient as a function of temperature and bias voltage is plotted in Figures 7 and 8.

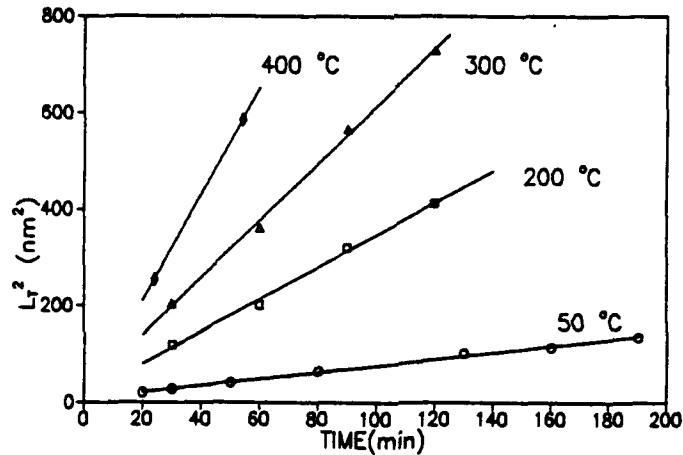


Figure 6. Growth law for four temperatures.

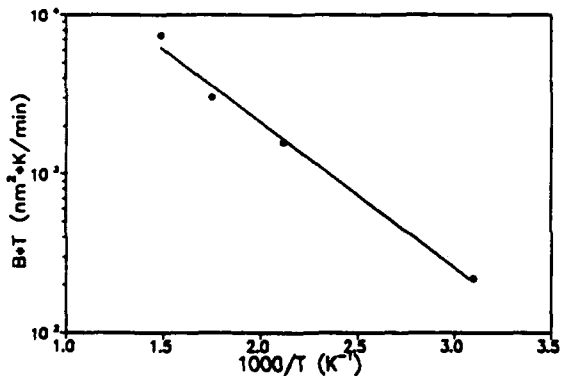


Figure 7. B vs. T.

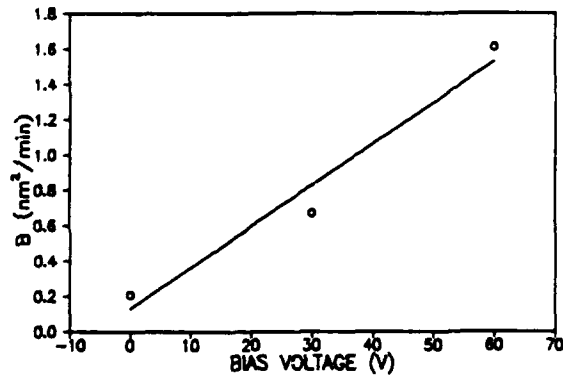


Figure 8. B vs. V.

The linear fit shown in Figure 7 yields an activation energy of 0.18 eV, which is notably lower than the activation energy for thermal oxidation (more than 1 eV¹⁶), and indicates a very different oxidation mechanism. The linear increase of the growth rate with the bias reveals that the oxidizing species are negative. Considering that in the ECR plasma the density of electrons is high, and consequently, the density of negative ions is low, a multistep process can be envisioned as was similarly reported for ECR formation

of thicker ECR grown oxides⁸. For the present situation we consider first that electrons in the plasma attach to oxygen producing the molecular ion, O_2^- . This species is less stable than O_2 , and will readily decompose to the atomic species O and O^- . The O^- can readily migrate through the oxide with a positive sample bias.

The best optical description of the interface layer was as a mixture of oxide and amorphous silicon. This description simulates the result of several phenomena: interface roughness, suboxides, and strained oxide. From our measurement we cannot decide which ones are dominant, but we know for sure that this interface layer is very different from a pure oxide and that its optical behavior is almost constant during plasma oxidation, hence this layer can be used as a marker. The immutability of this layer during the growth strongly suggests that the oxidation occurs between this layer and the outer surface. In this way oxidation occurs from the movement of both the Si outward as a cation and the oxidant species inward as O^- . In this hypothesis the interface layer is partly the result of the migration of Si^+ through the first layer of the oxide. Our previous study of the nature of this interface layer⁹ has shown that with positive or zero bias this layer is optically indistinguishable from the interface layer seen for thermally grown SiO_2 , and the recent Carl et al work⁸ has shown similar electrical quality for the positive and zero biased ECR oxide films with thermal oxides.

ACKNOWLEDGEMENTS

This work was supported in part by the Office of Naval Research, ONR, and the NSF Engineering Research Center at NC State Univ. One of us (J.J.) is grateful to NATO for a travel fellowship.

REFERENCES

1. J.R.Ligenza, *J.Appl.Phys.*, **36**, 2703 (1965).
2. V.Q. Ho and T. Sugano, *Jpn.J.Appl.Phys.*, **19**, 103 (1980).
3. R.P. Chang, C.C. Chang, and S. Darack, *Appl.Phys.Lett.* **36**, 399 (1980).
4. S. Kimura, E. Muraki, K. Miyake, T. Warabisako, H. Sunami and T. Tokuyama., *J.Electrochem.Soc.*, **132**, 1460 (1985).
5. T. Ropel, D.K. Reinhard, and J. Asmussen., *J.Vac.Sci. Technol. B*, **4**, 295 (1986).
6. C. Vinckier, P. Coeckelberghs, G. Stevens, M. Heyns, and De Jaegere., *J.Appl.Phys.*, **62**, 1450 (1987).
7. D.A. Carl, D.W. Hess, and M.A. Lieberman., *J.Vac.Sci.Technol. A*, **8**, 2924 (1990).
8. D.A. Carl, D.W. Hess, M.A. Liberman, T.D. Nguyen and R. Gronsky, *J. Appl. Phys.*, **70**, 3301 (1991).
9. Y.Z. Hu, J. Joseph , and E.A.Irene, *Appl.Phys.Lett.*, **59**, 1353 (1991).
10. J. Joseph, Y.Z. Hu, and E.A. Irene, *J.Vac.Sci.Technol.B*, **10**, Mar/Apr (1992).
11. J.W. Andrews, Y.Z. Hu, and E.A. Irene, *SPIE Proc.*, **1118**, 62 (1990).

12. J.W. Andrews, Ph.D Thesis , University of North Carolina. Chapel Hill, NC 1990.
13. D.E. Aspnes, Thin Solid Films, 89, 249 (1982).
14. D.E. Aspnes, and A.A. Studna., Phys. Rev. B, 27, 985 (1983).
15. D.E. Aspnes, A.A. Studna, and E. Kinsbron., Phys.Rev.B, 29, 768 (1984).
16. I.H. Malitson, J.Opt.Soc.Am., 55, 1205 (1965).
17. E.A. Irene, CRC Crit.Rev.Sol.State Mat. Sci., 14, 175 (1988).
18. N. Cabrera and N.F. Mott, Rep.Prog.Phys., 12, 163 (1948).